NJC

Accepted Manuscript

This article can be cited before page numbers have been issued, to do this please use: X. L. Xu, F. Hu and Q. Shuai, *New J. Chem.*, 2017, DOI: 10.1039/C7NJ03046K.

ROYAL SOCIETY OF CHEMISTRY

rsc.li/njc

View Article Online
DOI: 10.1039/C7NJ03046K

Journal Name

ARTICLE

A facile synthesis, crystal structure and bioactivity evaluation of two novel barium complexes based on 2,4,6-trichlorophenoxyacetic acid and *o*-ferrocenylcarbonyl benzoic acid

Received 00th January 20xx,
Accepted 00th January 20xx

DOI: 10.1039/x0xx00000x

www.rsc.org/

Xiuling Xu, Fan Hu and Qi Shuai*

Two novel Ba(II) complexes [Ba(**TCPA**)$_2$(H_2O)$_4$] **1** and [Ba(H_2O)$_8$]·2(***o*-FcCOC$_6$H$_4$COO**)·6H_2O **2** [**HTCPA** = 2,4,6-trichlorophenoxyacetic acid and ***o*-HOOCC$_6$H$_4$-COFc** = *o*-ferrocenylcarbonyl benzoic acid] have been synthesized by facile microwave method. The solid-state structures were well established by means of X-ray crystallography as well as routine analysis of infrared spectrum (FTIR), elemental analysis, field emission scanning electron microscope (FESEM) and thermogravimetric analysis (TG). Different polyhedron of tricapped triangular prism for **1** and dodecahedron for **2** were present. It's worth noting that central Ba(II) ion in **1** is nine-coordinated by two carboxylate oxygen atoms from **TCPA** ligands and seven oxygen atoms from coordinated water molecules. By contrast, the eight-coordinated Ba(II) in **2** forming barium-water clusters assembled by O-H···O hydrogen-bond contributed by coordinate water molecules. The uncoordinated ***o*-OOCC$_6$H$_4$-COFc** ligands in **2** play a key role in the process of charge balance. FESEM images exhibited different surface appearances between ligand and barium complexes, that is: flower-like **HTCPA**, branch-like ***o*-HOOCC$_6$H$_4$-COFc**, block-like complex **1** and corner-truncated cubes complex **2**. The allelopathic activity of the complexes and their corresponding ligands was evaluated against two herbaceous plants of barnyard grass and turnip (Raphanus sativus). All the tested compounds showed certain activity with good RI values. Antifungal bioassay was also carried out *in vitro* on three strains of *Botrytis cinerea* Pers., *Glomerella cingulata* Schr, and *Cytospora* sp. Complex **1** and **HTCPA** can against all the three tested fungus, while ***o*-HOOCC$_6$H$_4$-COFc** and **2** only worked for *Botrytis cinerea* Pers. The complex presented in this paper has potential applications in weed control, and this work provides an experimental basis for future studies on Ba-based pesticides.

Introduction

The need to increase world grain output for the rapidly growing population is well recognized. Pesticides, controlling weeds (barnyard grass, broadleaf weeds, cyperaceae weeds, etc.) and pathogens (Botrytis cinerea Pers., Cytospora sp., etc.), have contributed greatly to the boost farm income.[1, 2] However, for many years now, excessive use of pesticides has been one of the major causes of environment pollution, including air, water, soil and biological pollution.[3-8] More and more countries exert great efforts to develop highly efficient pesticides by structural modification of existing compounds (phenoxy carboxylic acids, sulfonyl, pyridazine, pyrazoles, triazolinones, uracils and triketones).[9-15] Without destroying the chemical structure of pesticides, coordination of herbicide molecules with metal ions is an effective way to improve efficiency.[16, 17] In recent years, a great number of novel efficient pesticides were synthesized in large quantities through the coordination method and achieved superior results compared with that of the single ligands.[18-21] For example, Lei's group in 2009 synthesized the triadimefon copper complex for the first time and proved that the inhibitory effect of the complex on *Rhizoctonia leges* and *Rhizoctonia solani* was better than that of the ligand.[22] A wide variety of metal centres have been employed to develop pesticides exhibiting satisfactory results, however, the study of Ba(II) remains largely unexplored. In fact, the toxicity of water-soluble barium compounds was caused by altering the cell membrane permeability through blocking K(I) channels.[23-27] The development of Ba-based pesticides might be an efficient method to enhance the pesticides activity.

The abovementioned structural modification that improved the efficiency of compounds was mainly based on coordination effect of bioactive ligands with O, S and N atoms to different metal centres. Chlorophenoxyacetic acid and ferrocene-based carboxylate are two kinds ligands with excellent bioactivity.[28-32] Since the USDA first

Shaanxi Key Laboratory of Natural Products & Chemical Biology, College of Chemistry & Pharmacy, Northwest A&F University, Yangling, Shaanxi 712100, People's Republic of China.
E-mail: shuaiqi@nwsuaf.edu.cn;

†Electronic supplementary information (ESI) available: UV-vis spectra of two complexes and ligands. ^{1}HNMR spectra of ligands. IR spectrum of complexes **1** and **2**. and some activity data. For ESI and crystallographic data in CIF or other electronic format See DOI:10.1039/x0xx00000x

View Article Online
DOI: 10.1039/C7NJ03046K

reported the herbicidal effect of 2,4-dichlorophenoxyacetic acid in 1944, more and more derivatives with advantages of high efficiency, low consumption and low cost have been developed in the world. As a kind of organochlorine herbicide, chlorophenoxyacetic acid usually inhibits the growth of hormones in plants by disrupting their normal level. On the other side, ferrocene, which was first discovered in 1951, has captured the imagination of chemists because of its fascinating sandwich structure and is considered among the important structural motifs in organometallic chemistry, materials science and herbicides. Incorporation of a ferrocene fragment into a molecule of an organic compound often obtained unexpected biological activity, which is attributed to their different membrane permeation properties and anomalous metabolism. Most interestingly, similar to chlorophenoxyacetic acid, ferrocenyl derivatives also possess a very high level of plant growth regulatory activity on a wide variety of crops.[33-39] From structural point of view, difficulties in synthesis of Ba(II) complexes caused by small charge and large radii would be improved by applying these two kinds of carboxyl group-containing ligands. The various coordination modes (Fig. 1) of carboxyl group provide high probability to achieve structural modification of Ba(II) on existing pesticides through coordination effect. Full utilization of the above-mentioned carboxyl group-containing ligands to build Ba(II) complexes for efficient herbicides is significant.

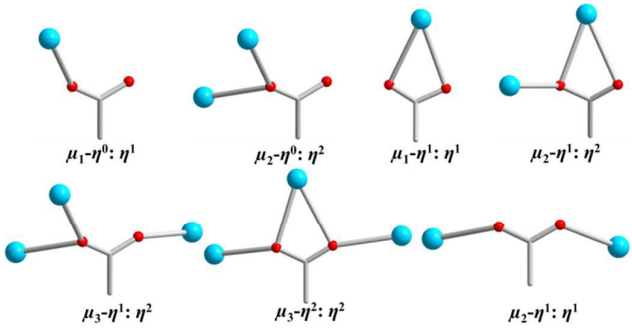

Fig. 1 The coordination modes of carboxyl.

Since the first discovery of the microwave by Percy Spencer in 1946, microwave radiation method has been widely applied to synthsize organic molecules, zeolites, nanoparticles, etc.[40-42] However, microwave synthesis has not been well applied to synthesize complexes compared to traditional solvent and hydrothermal method. Our previous works have successfully synthesized Mg(II), Ca(II), Sr(II) complexes through rapid microwave method.[43-46] This work was the deeper study about microwave method applied in Ba(II) complexes synthesize. Herein, two novel complexes $[Ba(\mathbf{TCPA})_2(H_2O)_4]$ **1** and $[Ba(H_2O)_8]\cdot 2(\boldsymbol{o}\text{-}\mathbf{FcCOC_6H_4COO})\cdot 6H_2O$ **2** [**HTCPA** = 2,4,6-trichlorophenoxyacetic acid and ***o*-HOOCC$_6$H$_4$-COFc** = *o*-ferrocenylcarbonyl benzoic acid] were synthesized for the first time. Their solid-state structures are well established by means of X-ray crystallography as well as routine analysis of infrared spectrum, elemental analysis, field emission scanning electron microscope and thermogravimetric analysis. Allelopathic activity of ligands and complexes with turnip (Raphanus sativus) and barnyard grass have been evaluated. The Antifungal bioassay on three strains, *Botrytis cinerea* Pers., *Glomerella cingulata* Schr, *Cytospora* sp were also reported.

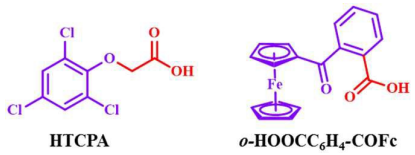

Scheme 1 Chemical structure of the **HTCPA** and ***o*-HOOCC$_6$H$_4$-COFc** ligands.

Experimental

2.1. Materials and physical measurements

2,4,6-trichlorophenol, ethyl chloroacetate, phthalic anhydride, aluminium chloride and ferrocene were purchased commercially from Aladdin Reagent Co. Ltd. (Shanghai, China). NMR spectra were recorded on a Bruker 500 MHz spectrometer with tetramethylsilane as an internal standard. Microwave synthesis was carried out on a CEM Discover SP single-mode microwave synthesis reactor. Elemental analyses (C and H) were performed on a Vario MACRO cube elemental analyzer. IR spectra were recorded on a BRUKER TENSOR 27 spectrophotometer within 400-4000 cm^{-1} using the samples prepared as pellets with KBr. Field emission scanning electron microscope measurements were performed on a FEI Nova Nano SEM 450 from Life Science Research Core Services (LSRCS) of Northwest A&F University. TG analysis was performed on a SHIMADZU TA-60ws from 25 to 1000 ^oC at a heating rate of 10 ^oC min^{-1} in N_2 atmosphere.

2.2. Synthesis of the ligands and complexes

2.2. 1. Synthesis of the ligand HTCPA

The ligands were prepared by the microwave reaction as shown in Scheme 2. In a microwave tube, 2.4.6-chlorophenol (5 mmol, 987 mg) was dissolved in dry N, N-dimethylformamide (2 mL) followed with 2 mL aqueous solution of K_2CO_3 (691.05 mg, 5 mmol), ethyl chloroacetate (5 mmol, 0.61 g) and KI (166 mg, 1 mmol). The reaction mixture was allowed to irradiate for 4 min at 100 ^oC under 200 W. Then 5 mL of NaOH (2 M) was added to the mixture and irradiated for 5 min at 150 ^oC under 500 W. The resulting solution was acidified (pH = 6) by adding of a 1 M hydrochloric acid solution under vigorous stirring after the mixture cooled to room temperature. The crude product was purified by column chromatography on silica gel using petroleum ether: ethyl acetate (4:1, v/v) as the eluent. Then **HTCPA** ligand as white solids was obtained. Yield: 83 %. Found ^1H NMR (DMSO/TMS, 500 MHz, ppm): δ 13.25 (s, 1H), 7.81 (s, 2H), 4.68 (s, 2H).

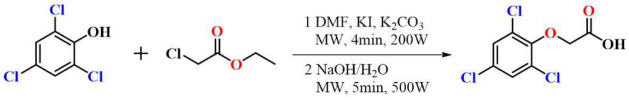

Scheme 2 Microwave synthesis of the **HTCPA** ligand.

2.2. 2. Synthesis of the ligand *o*-HOOCC$_6$H$_4$-COFc

In a 250 mL round-bottom flask, a mixture of phthalic anhydride (5.92 g, 40 mM) and aluminium chloride (10.67 g, 80 mM) in dichloromethane (80 mL) were stirred for 15 min under a nitrogen atmosphere at room temperature. Next, a solution of ferrocene (7.44 g, 40 mM) dissolved in CH_2Cl_2 (80 mL) was added dropwise in 30

View Article Online
DOI: 10.1039/C7NJ03046K

min. After refluxed for 4 h, the resulting mixture was diluted with 2 M hydrochloric acid solution (25 mL) and the organic layer was separated, then the aqueous layer was extracted with CH_2Cl_2. The combined organic layers were dried over anhydrous $MgSO_4$ and concentrated under reduced pressure. The crude product was purified by column chromatography on silica gel using petroleum ether: ethyl acetate (6:1, v/v) as the eluent. Then ***o*-HOOCC$_6$H$_4$-COFc** ligand was obtained as a yellow solid. Yield: 76 %. Found ^{1}H NMR ($CDC1_3$/TMS, 500 MHz, ppm): δ 8.04 (s, 1H), 7.68 (d, J = 23.4 Hz, 2H), 7.61 – 7.52 (m, 1H), 4.62 (s, 2H), 4.55 (s, 2H), 4.22 (s, 4H).

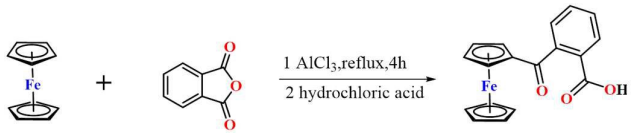

Scheme 3 Microwave synthesis of the ***o*-HOOCC$_6$H$_4$-COFc** ligand.

2.2. 3. Synthesis of compounds [Ba(TCPA)$_2$(H$_2$O)$_4$] 1

An appropriate amount of NaOH solution (0.2 mM, 0.5 mL) was added dropwise to **HTCPA** ethanol solution (0.2 mM, 0.5 mL) under stirring to adjust the pH value to approximately 7. Then the $BaCl_2 \cdot 2H_2O$ (0.1 mmol, 24.43 mg) dissolved in distilled water (5 mL) was added into this mixture under stirring with the molar ratio of Ba^{2+}: **HTCPA** = 1 : 2. Finally, the mixture was transferred into a 25 mL microwave tube. The mixture was heated by microwave at 100 ^oC for 1 h at 140 W and then cooled to room temperature, continued to be cultivated by slowly evaporating the filtrate at room temperature. The colorless, block crystals (Fig. 2(1)) suitable for X-ray diffraction were obtained. Yield: 32 %, based on Ba. Anal. calc. for $BaC_{16}H_{16}Cl_6O_{10}$: C, 26.73; H, 2.23 %. Found: C, 26.77; H, 2.31 %. IR data (cm^{-1}): ν(O-H): 3279 b; ν_{asym}(COO^-): 1734 s; ν_{sym}(COO^-): 1709 s; ν(Ar-O-C): 1461 s, 1425 s, 1141, 1084 s; ν(-CH_2-): 672 m.

2.2. 4. Synthesis of compounds [Ba(H$_2$O)$_8$]·2(*o*-FcCOC$_6$H$_4$COO)·6H$_2$O 2

For the preparation of complexes **2**, 5 mmol of ***o*-HOOCC$_6$H$_4$-COFc** and deionized water (10 mL) were placed together in a 25 mL microwave tube, and deprotonated by adding NaOH (0.2 mM) until the pH=7. After the vigorous stirring for five minutes, 0.25 mmol of $BaCl_2 \cdot 2H_2O$ added. Then the mixture was heated by microwave under autogenous pressure at 100 ^oC for 1 h at 200 W and cooled to room temperature. The crystal was obtained by slowly evaporating the filtrate at room temperature. The red-brown, block crystals (Fig. 2(2)) suitable for the X-ray diffraction were obtained directly on the filter paper. Yield: 78 %, based on Ba. Elemental analysis calcd. (%) for $BaC_{36}H_{54}Fe_2O_{20}$: C, 40.92; H, 5.11. Found: C, 40.91; H, 5.13. IR (KBr, cm^{-1}): ν(O-H): 3448 s, 3065 m; ν_{asym}(COO^-): 1695 s, ν_{sym}(COO^-): 1584 m; ν(Ar): 1448 s, 1393 m, 1293 s, ν(ferrocene): 1121 s, 931s, 754 s, 653 s, 481 s.

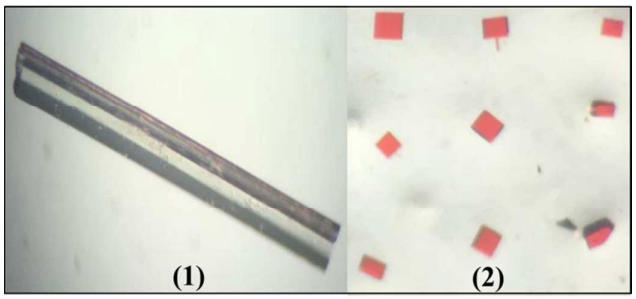

Fig. 2 Crystals images of complexes **1** and **2**.

2.3. Single-crystal X-ray structure determinations

All crystallographic data were collected on a Bruker SMART CCD area-detector diffractometer at 298(2) K with graphite monochromatized Mo-Kα radiation (λ = 0.71073 Å) in ω scan mode, the data reduction was performed using Bruker SAINT. The crystal structures were resolved by direct methods and refined with full-matrix least-squares refinement on F^2 with anisotropic displacement parameters for non-H atoms using SHELXTL.[47] All atoms were refined geometrically. Structural plots were generated with Diamond. A summary of crystallographic data for **1** and **2** is presented in Table S1. Bond lengths (Å) and angles (°) of bond for **1** and **2** are given in Table S2. Crystallographic data have been deposited with the Cambridge Crystallographic Data Centre, CCDC number 1546818 for **1**, 940743 for **2**. These data can be obtained free of charge *via* www.ccdc.can.ac.uk/conts/retrieving.html (or from the Cambridge Crystallographic Centre, 12 Union Road, Cambridge CB2 1EZ, U.K., fax (+44) 1223-336033, or deposit@ccdc.cam.ac.uk).

2.4. Allelopathic Bioassay

The seeds of two herbaceous plants, barnyard grass and turnip (Raphanus sativus), were used for the bioassay. The procedure was conducted according to the following steps. The plant seeds were washed with running water for 2 h, soaked in 0.3 % $KMnO_4$ for 15 min, flushed until they were colorless. The compounds, positive control (glyphosate) and blank solvent methanol, were added to 12-well plates with filter paper to serial concentration gradient of 50–200 ppm. After the evaporation of methanol, the plant seeds were sown in the micro dishes and irrigated with deionized water. Triplicate experiments were conducted. The plates were incubated at 24 °C for 90 h. The germination rates were calculated according to eq 1, and allelopathic effects [response index (RI)] were calculated according to eq 2.

germination rate (%)= (number of germinated seeds)/ (total number of seeds) 1)

If $T > C$, then RI = $1 - C / T$; if $T < C$, then RI = $T / C - 1$ 2)

Where T is the length of the treatment, C is the length of the blank control, and RI is the response index.

2.5. Antifungal bioassay

View Article Online
DOI: 10.1039/C7NJ03046K

The tested phytopathogenic fungi (*Botrytis cinerea* Pers, *Glomerella cingulata* Schr, *Cytospora* sp) were provided by Shaan xi Key Laboratory of Natural Products & Chemical Biology, College of Chemistry & Pharmacy, Northwest A&F University. The tested fungi were maintain cultured on potato dextrose agar (PDA) slants at 4 °C and subcultured in Petri dishes prior to testing. The *in vitro* antifungal activity of the tested compounds was evaluated by the mycelial growth inhibitory rate method. Solutions of each compound were prepared by dissolving the appropriate amount of compound in acetone. Equal volumes of acetone containing diluted compounds were added to sterile cool agar media (PDA) to give suitable concentrations for each substance. A zero-concentration treatment (control plate), containing the same percentage of acetone to ensure equivalent concentrations of these components in all the treatments, was prepared for each strain. The final acetone concentration did not exceed 0.5 % of the final volume in both control and treated cultures. Compound-amended agar medium was dispersed aseptically onto 9-cm-diameter glass Petri dishes (10 mL/dish). Each dish was inoculated with three mycelial discs (4 mm diameter) cut from the periphery of actively growing colonies. Three replicate plates for each fungus were incubated at 28 (±2) °C for all test fungi. Control plates containing media mixed with acetone (1 mL) were included. Having cultured for 60 h, the mycelial growth of fungi (mm) in both treated (*T*) and control (*C*) Petri dishes was measured diametrically in two different directions (decussation method) till the fungal growth in the control dishes was almost complete. The percentage of growth inhibition (*I*) was calculated according to eq 3.

$$I\,(\%) = [(C\text{-}T)/C]\cdot 100 \qquad 3)$$

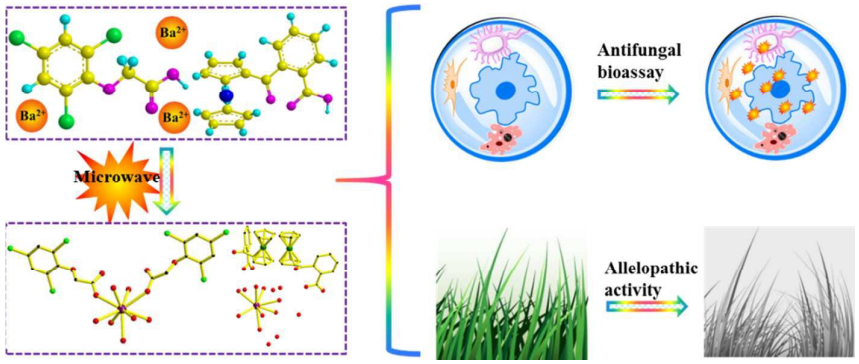

Scheme 4 Schematic illustration of microwave synthesized complexes used for bacteriostat and herbicides.

3. Results and Discussion

3.1. Structural description for 1 and 2

3.1.1. The crystal structure of $[Ba(TCPA)_2(H_2O)_4]$ 1

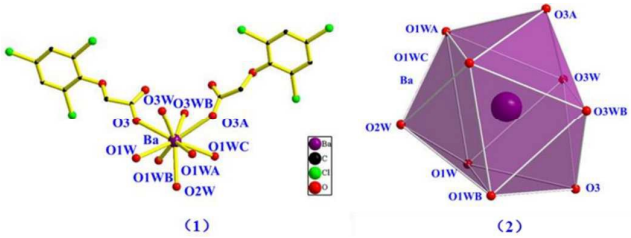

Fig. 3 The coordination environment and coordination polyhedron of Ba(II) in **1**.

Single-crystal X-ray diffraction analysis reveals that **1** crystallizes in Orthorhombic crystal system, *Pbcm* space group. The coordination environment and coordination polyhedron of Ba(II) is presented with atom numbering scheme (Fig. 3). The asymmetric unit consists of one crystallographically independent Ba(II) ion, two **TCPA** ligands and four coordinated water molecules. The central Ba (II) ion exhibiting a tricapped triangular prism coordination geometry, with the caps (O2W, O3A, O3) of the three plane construct by the oxygen atoms of O1W-O1WB-O1WC-O1WA, O1WA-O1WC-O3WB-O3W and O3W-O3WB-O1WB-O1W. The central Ba (II) ion is nine-coordinated by two carboxylate oxygen atoms (O3, O3A) from two **TCPA** ligands and seven oxygen atoms (O1W, O1WA, O1WB, O1WC, O2W, O3W, O3WB) from coordinated H_2O molecules. The length of the Ba−O bonds range from 2.718(7) to 2.953(6) Å, with the average value of 2.824 Å. The crystal structure of $[Ba(\mathbf{TCPA})_2(H_2O)_4]$ shows that the compound is a one-dimensional polymer with $[Ba(\mathbf{TCPA})_2(H_2O)_7]$ repeat units. The repeat unit is infinitely extended along the *a*-axis crystallographic direction to generate a metal-based 1D chain, as shown in Fig. S6. An interesting structural feature for the 1D chains is all of the Ba(II) ions lie on a straight line. The lengths of the two neighboring Ba(II) ions are d=4.2229 Å, and the Ba···Ba···Ba torsion angle for the wings is α=180 (Fig. S6).

The coordination of **TCPA** ligands involves carboxylato oxygen atoms in one coordination modes in each dimeric unit. The **TCPA** ligands act as monodentate ligands bound to the Ba(II) atom through O(3) atom，and the Ba-O bond length was d= 2.76Å. Each 1D chain was linked by hydrogen bonds to form a 2-D layered network in *ab*-plane of the cell in which the **TCPA** ligands point alternately up and down (Fig. S7). Neighboring layered networks are further connected into a 3-D supramolecular framework through van der waals forces (Fig. S8).

3.1.2. The crystal structure of $[Ba(H_2O)_8]\cdot 2(o\text{-}FcCOC_6H_4COO)\cdot 6H_2O$ 2

X-ray diffraction reveals that complex **2** is a co-crystal structure and crystallizes in the triclinic crystal system with the space group of *P*-1. There are one crystallographically independent Ba(II) ion, two ***o***-

View Article Online
DOI: 10.1039/C7NJ03046K

OOCC$_6$H$_4$-COFc ligands, eight coordinated water molecules and six lattice water (O15, O16, O17, O18, O19, O20) in the asymmetric unit. One Ba(II) ion and eight water molecules (O7, O8, O9, O10, O11, O12，O13, O14) form the barium-water clusters $[Ba(H_2O)_8]^{2+}$ with the Ba−O distance ranging from 2.69(2) to 2.890(11) Å which is in agreement with other complexes containing Ba(II) centers (Fig. 7), and the co-crystal structure formed by ***o*-OOCC$_6$H$_4$-COFc** and $[Ba(H_2O)_8]^{2+}$ in ratio of 2:1.

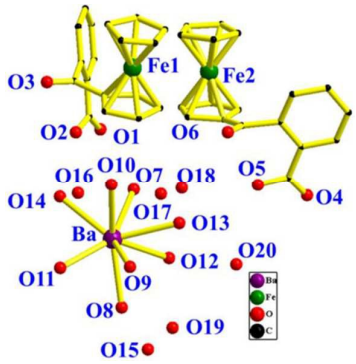

Fig. 4 The coordination environment of Ba(II) in **2**.

The coordination polyhedron around the Ba(II) atom could be best described as dodecahedron arrangement which constructed by O11-O8-O14, O8-O11-O9, O9-O11-O10, O10-O11-O14, O14-O10-O7, O8-07-O14, O8-O7-O12, O13-O10-O7, O7-O12-O13, O12-013-O8, O9-O13-O10 and O8-O13-O9. (Fig. 5).

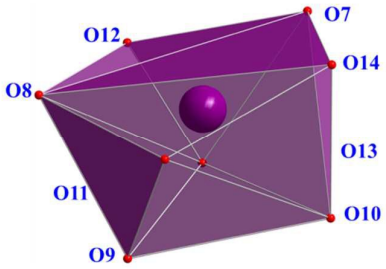

Fig. 5 The coordination polyhedron of Ba(II) in **2**.

For complex **2**, although the ***o*-OOCC$_6$H$_4$-COFc** anions did not direct coordinated with Ba(II) atom, but hydrogen bond interactions between $[Ba(H_2O)_6]^{2+}$ and -COO$^-$ of ferrocenyl carboxyl (Fig. S9.) played an important role in the formation of sandwich 1D chains structure with ligand anions as outer layer and centre metal cation as interlayer along *b*-axis. The uncoordinated ***o*-OOCC$_6$H$_4$-COFc** molecules play an important role of balancing the charge, and they also bridge the neighboring Ba(II) by the formation of hydrogen bonds between coordinated water molecules and carboxyl oxygen atoms.

The adjacent 1D linear chains are self-assembled to form a 2D supramolecular layer with the π…π stacking interactions along the *ab* plan (Fig. S10). Neighboring layered networks are further connected into a 3-D supramolecular framework through van der waals forces (Fig. S11).

3.1.3. Structures comparison of complex 1 and 2

Complex **1** and **2**, derived from two kinds of carboxylic acid ligands, both have many similarities and own structural features. In each asymmetric unit contain one Ba(II), two ligands and different numbers of coordinated water molecules. Different coordination polyhedron was present in these two complexes (tricapped triangular prism corresponds to coordination numbers 9 in **1**, while dodecahedron arrangement corresponds to coordination numbers 8 in **2**). It is interesting to note, that the Ba(II) in **2** forming barium-water clusters with coordinate water rather than coordinate to ***o*-OOCC$_6$H$_4$-COFc** ligands, so a co-crystal structure presented. The structure analysis show that weak interaction play an important role in forming the multidimensional structure, such as 1D chains is linked by hydrogen bonds to form a 2-D layered in **1**, while the adjacent 1D linear chains are self-assembled to form a 2D supramolecular layer with the π…π stacking interactions along the *ab* plan in **2**.

3.2.Thermogravimetric analysis of complexes 1 and 2

The TG-DTG analysis curves recorded reveals that the structures of complexes show different thermal decomposition behavior (Fig. 6). TG-DTG curves of **1** and **2** were measured at the heating rate of 10 ^oC min^{-1} in the temperature range from 25 to 1000 ^oC under the N_2 atmosphere. For the first step, in the ranges of 25 ^oC–243.89 ^oC, complex **1** lost four coordinated water molecules (The experimental mass loss was 15.956 %; the calculated mass loss was 13.675 %), the DTG trace gives one endothermic peak at 137.22 °C (Fig. 6(1)). And for complex **2**, in the ranges of 25 ^oC–217.38 ^oC for the loss of eight coordinated water and six lattice water (the experimental mass loss was 23.843 %; the calculated mass loss was 23.867 %), on the DTG curve，the peak temperatures was 148.38 ^oC (Fig. 6(2)). For compound 1，in the subsequent steps, there is another 54.762 % (calculated 57.204 %) weight loss up to 1000 ^oC. These weight losses are due to the complete decomposition of the compound and leaving the residues of BaO (observed 29.282 %; calculated 29.121 %)，the DTG curve shows that there are one peaks at 337.49 ^oC. For complex **2**, following decomposition belongs to the continuous collapse of the frameworks with a value of 61.349 % (Calcd. 61.613 %) at the temperature range of 217.21–1000 ^oC, the DTG curve shows that there are one peaks at 519.40 ^oC in the temperature range of 496.179–573.48 ^oC. To the end, the complex is completely degraded into $BaO(FeO)_2$ (observed 14.808 %; calculated 14.522 %) for **2** after the final decomposition.

View Article Online
DOI: 10.1039/C7NJ03046K

Journal Name

ARTICLE

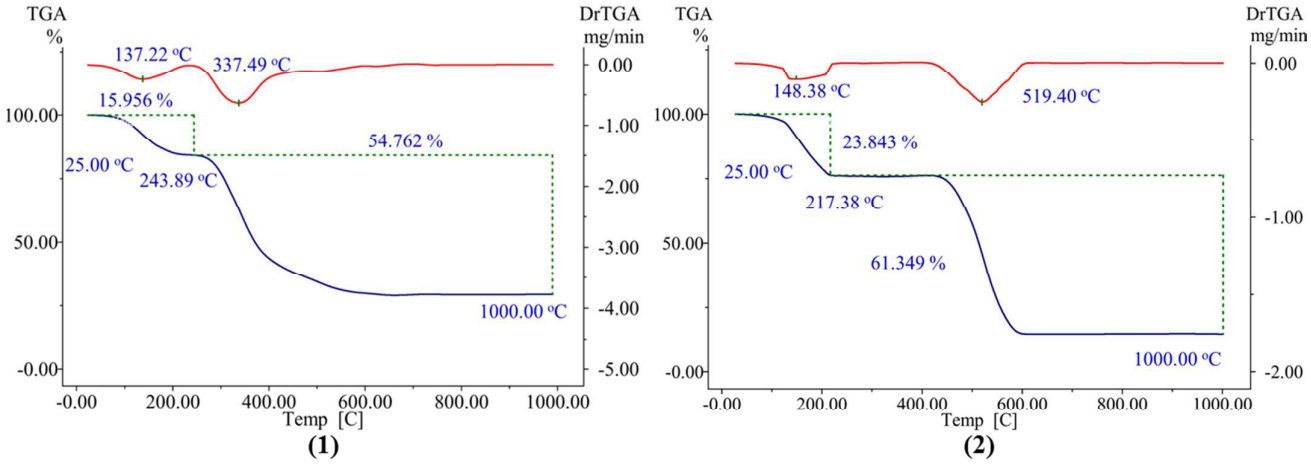

Fig. 6 TG and DTG curves of the complexes **1** and **2**.

3.3. FESEM characterizing of Ligands and complexes

The FESEM images of **HTCPA**, complex **1**, ***o*-HOOCC$_6$H$_4$-COFc** and complex **2** are shown in Fig. 7. The **HTCPA** were flower-liked. However, after coordinated, the complex **1** change to homogeneous clumpy-liked sheets with the smooth surface. Similarly, a distinct change in morphology from shaly bedded to corner-truncated cubes was observed upon addition of Ba(II) ion to the solution containing ***o*-HOOCC$_6$H$_4$-COFc** ligands.

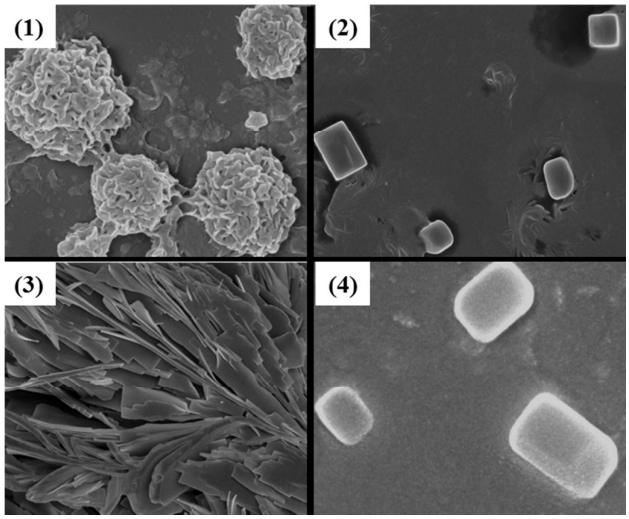

Fig. 7 FESEM images of the ligands and complexes. (1) FESEM images for **HTCPA**, (2) FESEM images for complex **1**, (3) FESEM images for ***o*-OOCC$_6$H$_4$-COFc** and (4) FESEM images for complex **2**.

3.4. Evaluation of Allelopathic Activity

All isolated compounds were evaluated for allelopathic activity against barnyard grass and turnip (Raphanus sativus) using our previously reported assay by determining the germination rates and seedling growth (root and shoot elongation) with respect to the control, glyphosate, a broad-spectrum systemic herbicide. The RI was selected as an evaluation indicator, which ranges from −1 to 1, with positive values indicating stimulation by the treatments and negative values indicating inhibition by them, the RI was considered to be superior to the *T*/*C* statistical method and easy to interpret because it is simply the proportional reduction of the treatment relative to the control. As shown in Table 3, whether the complexes or ligands can inhibit the elongation of barnyard grass, while most being less active than the positive control glyphosate.With the increase of the solution concentration, moderate to strong growth inhibitory effects (shoot elongation and root elongation) were observed for all of the compounds.

In general, 2,4,6-trichlorophenoxyacetic acid demonstrated stronger inhibitory activity than that of the complex **2**. In particular, **HTCPA** showed the prominent inhibition of shoot and root elongation (-0.32~-0.41 and -0.33~-0.47, respectively) at 50~200 ppm compared to those of the control glyphosate (-0.31~-0.39 and -0.31~-0.43, respectively). In contrast, ***o*-OOCC$_6$H$_4$-COFc** and **2** containing a benzoyl side chain and a ferrocene group showed weaker inhibition. However, complex **2** are more superior than ***o*-OOCC$_6$H$_4$-COFc** ligand. Our results revealed that all administered experimental agents, caused a dose-dependent inhibition of seedling growth. The overall observed growth inhibitory effects order revealed to be the following: **HTCPA** > **1** > **2** > ***o*-OOCC$_6$H$_4$-COFc**.

View Article Online
DOI: 10.1039/C7NJ03046K

Journal Name

ARTICLE

Table 1 Allelopathic Effects on barnyard grass of ligand and complexes **1** and **2**

Compound	Germination rate				Shoot elongation（RI）				Root elongation（RI）			
	50	100	150	200	50	100	150	200	50	100	150	200
HTCPA	0.72	0.67	0.72	0.72	-0.32	-0.36	-0.39	-0.41	-0.33	-0.37	-0.41	-0.47
1	0.94	0.89	0.72	0.94	-0.28	-0.31	-0.32	-0.35	-0.24	-0.26	-0.30	-0.37
***o*-OOCC$_6$H$_4$-COFc**	0.50	0.55	0.61	0.56	-0.18	-0.20	-0.27	-0.30	-0.21	-0.24	-0.26	-0.32
2	0.72	0.83	0.61	0.78	-0.21	-0.23	-0.28	-0.33	-0.23	-0.25	-0.27	-0.34
Gp	0.50	0.61	0.72	0.89	-0.31	-0.34	-0.37	-0.39	-0.31	-0.34	-0.40	-0.43
Ck	0.50	0.44	0.89	0.83								

3.5. Evaluation of Antifungal bioassay

Preliminary *in vitro* screening results of the title compounds for antifungal activities against three phytopathogenic fungi (*Botrytis cinerea* Pers., *Glomerella cingulata* Schr，*Cytospora* sp.) are listed in Table 2. The results indicated that some of the synthetic compounds exhibited over 25.90 % growth inhibition against mycelial growth of these tested fungi at concentrations of 100 mg/L.

The determined *I* values revealed that both ligands and complexes are active against *Botrytis cinerea* Pers and the complexes are more active than the ligands. It is noteworthy that the *I* values of complex **1** were 14.29, and **2** were 19.00, respectively, indicating that complex **2** possesses better activities than **1**. In fact, the main difference between **1** and **2** is that there are three substituted chlorine atoms on the ligand in **1** while ferrocene benzoyl in **2**. As one kind of organic chloride fungicides, similar to 2,4-dichlorophenoxyacetic acid, **TCPA** will attack proteins of *Botrytis cinerea* Pers. In the conditions that the concentration was 100 mg/L, the ***o*-OOCC$_6$H$_4$-COFc** and **2** resulted inactive against *Glomerella cingulata* Schr (-0.51 and -0.69) and *Cytospora* sp. (-3.97 and -5.02), whereas **HTCPA** and **1** show a moderate antibacterial activity (23.47, 25.90, 5.59, 6.65 respectivly). In fact, ferrocene has certain biological compatibility, at low concentrations, meanwhile the optimum concentrations was 100mg/L and rich Ba(II) couldpromote the growth of *Glomerella cingulata* Schr and *Cytospora* sp. As an overall result, compounds **HTCPA** and **1** resulted active against all the tested fungus. While ***o*-HOOCC$_6$H$_4$-COFc** and **2** only worked for *Botrytis cinerea* Pers but not for *Glomerella cingulata* Schr, *Cytospora* sp. Although the activity of the two complexes is weaker than the positive control, we still hope that the experimental results can provide a reference for peers and encourage more chemist to develop efficient antibacterial agents.

Table 2 Growth Inhibition [%] of three plant pathogenic fungi by ligands and complexes (conc. 100 mg/L)

Compound	*Botrytis cinerea* Pers.	*Glomerella cingulata* Schr	*Cytospora* sp.
HTCPA	17.43	23.47	5.59
1	19.00	25.90	6.65
***o*-HOOCC$_6$H$_4$-COFc**	13.21	-0.51	-3.97
2	14.29	-0.69	-5.02
Carbendazim	78.91	89.93	84.71

Conclusions

In summary, we presented two Ba(II) complexes based on **HTCPA**, ***o*-HOOCC$_6$H$_4$-COFc** and characterized their structures by X-ray diffraction methods, IR, elemental analysis, field emission scanning electron microscope and thermogravimetric analysis. In complex **1**,

View Article Online
DOI: 10.1039/C7NJ03046K

the central Ba (II) ions is nine-coordinated by two carboxylate oxygen atoms and seven oxygen atoms from coordinated H_2O molecules, while compound **2** coordinates to eight oxygen atoms which come from coordinated H_2O molecules. The carboxyl group of **HTCPA** in **1** exhibits monodentate coordination mode, and the uncoordinated ***o*-OOCC$_6$H$_4$-COFc** ligands in **2** play a key role in the process of charge balance. The title complexes **1** and **2** can also self-assemble to 3D network from 2D layers. FESEM images indicate that the ligand's surface appearance changed dramatically after coordination with Ba(II), such as flower-like for **HTCPA**, clump-like for complex **1**, shaly bedded for ***o*-HOOCC$_6$H$_4$-COFc** ligands and corner-truncated cubes for complex **2**. The results of allelopathic bioassay in this paper revealed that the activity of complex **2** was improved compared with single ***o*-HOOCC$_6$H$_4$-COFc** ligand (at the concentration range of 50–200 ppm, the RI values of shoot elongation was -0.21, -0.23, -0.28, and -0.33; the RI values of root elongation were -0.23, -0.25, -0.27, and -0.34). Further, to verify the antibacterial activity of the two complexes, antifungal bioassay was also carried out *in vitro* on the three strains of *Botrytis cinerea* Pers., *Glomerella cingulata* Schr. and *Cytospora* sp. Complex **1** and **HTCPA** can inhibit all the three tested fungus, whereas ***o*-HOOCC$_6$H$_4$-COFc** and **2** only worked for *Botrytis cinerea* Pers.

Acknowledgements

The authors gratefully acknowledge the financial supports from the National Natural Science Foundation of China (Grant No. 21473136, Grant No. 21103140).

Notes and references

1. A. Mkindi, N. Mpumi, Y. Tembo, P. C. Stevenson, P. A. Ndakidemi, K. Mtei and S. R. Belmain, *Ind. Crop. prod*., 2017,. doi: 10.1016/j.indcrop.2017.06.002.
2. G. Agoramoorthy, *Futures*, 2008, **40**, 503-506.
3. I. G. Dubus, J. M. Hollis and C. D. Brown, *Environ. Pollut*., 2000, **110**, 331-344.
4. P. C. Abhilash and N. Singh, *J. Hazard Mater*., 2009, **165**, 1-12.
5. V. F. Garry, *Toxicol Appl. Pharm*., 2004, **198**, 152-163.
6. R. Cochran, *Handbook of pesticide toxicology*, 2001, 691-704.
7. C. Bedos, P. Cellier, R. Calvet, E. Barriuso and B. Gabrielle, *Agronomie*, 2002, **22**, 21-33.
8. R. W. MacDonald, L. A. Barrie, T. F. Bidleman, M. L. Diamond, D. J. Gregor, R. G. Semkin, W. Strachan, Y. F. Li, F. Wania, M. Alaee, L. B. Alexeeva, S. M. Backus, R. Bailey, J. M. Bewers, C. Gobeil, C. J. Halsall, T. Harner, J. T. Hoff, L. Jantunen, W. L. Lockhart, D. Mackay, D. Muir, J. Pudykiewicz, K. J. Reimer, J. N. Smith, G. A. Stern, W. H. Schroeder, R. Wagemann and M. B. Yunker, *Sci. Total Environ*., 2000, **254**, 93-234.
9. L. Zheng, R. Wu, W. Guo, W. You, Y. Ling and X. Fan, *Chinese Chem. Lett*., 2015, **26**, 1008-1010.
10. X. Yu, Y. Liu, Y. Li and Q. Wang, *J. Agr. Food Chem*., 2016, **64**, 3034-3040.
11. S. F. McCann, G. D. Annis, R. Shapiro, D. W. Piotrowski, G. P. Lahm, J. K. Long and B. M. Reeves, *Synthesis and biological activity of oxadiazine and triazine insecticides: the discovery of indoxacarb,* 2002, 166-177.
12. J. P. Ma, Z. D. Yao, L. W. Hou, W. H. Lu, Q. P. Yang, J. H. Li and L. X. Chen, *Talanta*., 2016, **161**, 686-692.
13. S. A. Elmarakby, D. Supplee and R. Cook, *J. Agr. Food Chem*., 2001, **49**, 5285-5293.
14. A. Palasz and D. Ciez, *Eur. J. Med. Chem*., 2015, **97**, 582-611.
15. E. Jeong, M. Kim and H. Lee, *Pest Manag. Sci*., 2009, **65**, 327-331.
16. C. Dendrinou-Samara, L. Alevizopoulou, L. Iordanidis, E. Samaras and D. P. Kessissoglou, *J. Inorg. Biochem*., 2002, **89**, 89-96.
17. R. P. Sharma, A. Saini, J. Kumar, S. Kumar, P. Venugopalan and V. Ferretti, *Inorg. Chim. Acta*., 2017, **457**, 59-68.
18. F. Gozzo, G. Pizzingrilli and C. Valcamonica, *Pestic. Biochem. Phy.*, 1988, **30**, 136-141.
19. C. Marzano, M. Pellei, D. Colavito, S. Alidori, G. G. Lobbia, V. Gandin, F. Tisato and C. Santini, *J. Med. Chem*., 2006, **49**, 7317-7324.
20. K. J. Kilpin, S. Crot, T. Riedel, J. A. Kitchen and P. J. Dyson, *Dalton Trans.*, 2014, **43**, 1443-1448.
21. S. Sayen, A. Carlier, M. Tarpin and E. Guillon, *J. Inorg. Biochem*., 2013, **120**, 39-43.
22. M. K. Lei, P. Z. Zhang and Z. H. Zhong, *Agrochemicals*, 2008, **47**, 337-338.
23. L. Zheng, G. Liang, A. Gu, L. Yuan and Q. Guan, *J. Mater .Chem. C*., 2016, **4**, 10654-10663.
24. P. Diaz, C. Vallejos, I. Guerrero and G. Riquelme, *Placenta*., 2008, **29**, 883-891.
25. J. B. Park, H. J. Kim, P. D. Ryu and E. Moczydlowski, *J. Gen. Physiol*., 2003, **121**, 375-397.
26. Y. Sohma, A. Harris, C. J. Wardle, B. E. Argent and M. A. Gray, *Biophys. j.*, 1996, **70**, 1316-1325.
27. Y. X. Jiang and R. MacKinnon, *J. Gen. Physiol*., 2000, **115**, 269-272.
28. C. Zhu, L. Yang, D. Li, Q. Zhang, J. Dou and D. Wang, *Inorg. Chim. Acta*., 2011, **375**, 150-157.
29. K. Senthilkumar, M. Gopalakrishnan and N. Palanisami, *Spectrochim Acta. a*., 2015, **148**, 156-162.
30. J. Pinkas, Z. Bastl, M. Slouf, J. Podlaha and P. Stepnicka, *New J. Chem*., 2001, **25**, 1215-1220.

View Article Online
DOI: 10.1039/C7NJ03046K

31. M. L. Sun, B. F. Ruan, Q. Zhang, Z. D. Liu, S. L. Li, J. Y. Wu, B. K. Jin, J. X. Yang, S. Y. Zhang and Y. P. Tian, *J. Organomet. Chem*., 2011, **696**, 3180-3185.

32. C. Dendrinou-Samara, G. Psomas, C. P. Raptopoulou and D. P. Kessissoglou, *J. Inorg. Biochem*., 2001, **83**, 7-16.

33. H. C. Kawato, K. Nakayama, H. Inagaki, R. Nakajima, A. Kitamura, K. Someya and T. Ohta, *Org. Lett*., 2000, **2**, 973-976.

34. H. Yu, L. Shao and J. Fang, *J. Organomet. Chem*., 2007, **692**, 991-996.

35. Z. Jin, Y. Hu, A. Huo, W. Tao, L. Shao, J. Liu and J. Fang, *J. Organomet. Chem*., 2006, **691**, 2340-2345.

36. J. B. Liu, L. C. Li, H. Dai and J. X. Fang, *Appl. Organomet. Chem*., 2008, **22**, 237-241.

37. Y. S. Xie, X. H. Pan, B. X. Zhao, J. T. Liu, D. S. Shin, J. H. Zhang, L. W. Zheng, J. Zhao and J. Y. Miao, *J. Organomet. Chem*., 2008, **693**, 1367-1374.

38. Y. S. Xie, H. L. Zhao, H. Su, B. X. Zhao, J. T. Liu, J. K. Li, H. S. Lv, B. S. Wang, D. S. Shin and J. Y. Miao, *Eur. J. Med. Chem*., 2010, **45**, 210-218.

39. I. Damljanovic, M. Vukicevic, N. Radulovic, R. Palic, E. Ellmerer, Z. Ratkovic, M. D. Joksovic and R. D. Vukicevic, *Bioorg. Med. Chem. Lett*., 2009, **19**, 1093-1096.

40. P. Lidstrom, J. Tierney, B. Wathey and J. Westman, *Tetrahedron*, 2001, **57**, 9225-9283.

41. R. C. Hoffmann, S. Sanctis, E. Erdem, S. Weber and J. J. Schneider, *J. Mater. Chem. C*., 2016, **4**, 7345-7352.

42. M. Ghasemi, H. Javadian, N. Ghasemi, S. Agarwal and V. K. Gupta, *J. Mol. Liq*., 2016, **215**, 161-169.

43. X. L. Xu, S. S. Yan, F. Hu, W. Zhao and Q. Shuai, *J. Coord. Chem*., 2016, **69**, 541-550.

44. X. Xu, Y. Lu, L. Xu, F. Xie, Z. Pei and Q. Shuai, *J. Therm. Anal. Calorim*., 2015, **119**, 2053-2062.

45. X. Xu, F. Hu, S. Yan, J. Lin, Q. Li and Q. Shuai, *Rsc. Adv*., 2016, **6**, 67610-67618.

46. X. L. Xu, Y. H. Lu, F. Hu, L. T. Xu and Q. Shuai, *J. Coord. Chem*., 2016, **69**, 3294-3302.

47. G. M. Sheldrick, *Acta Crystallogr., Sect. C-Cryst. Struct.*, 2015, **71**, 3-8.

View Article Online
DOI: 10.1039/C7NJ03046K

A table of contents entry.

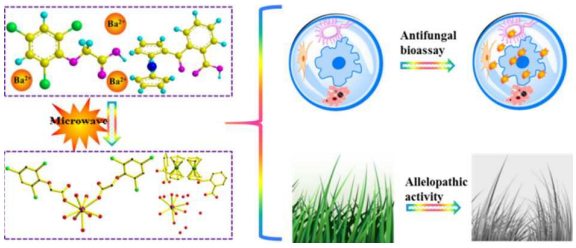

With a microwave method， two novel Ba(II) complexes were first synthesized and their allelopathic and antifungal activity evaluated.